PRODUCTION AND PROPERTIES OF COMPOSITES BASED ON CARBON NANOTUBE FIBRES

B. Mas[†1], J.J. Vilatela[*1]

[1] *IMDEA Materials Institute, Eric Kandel 2, Getafe 28906, Madrid, Spain*
[†] *Presenting Author: bartolome.mas@imdea.org*
[*] *Corresponding Author: juanjose.vilatela@imdea.org*

Keywords: CNT, Fibre, Composite

Abstract
Macroscopic carbon nanotube fibres spun from the gas phase during CNT growth were integrated into thermoplastic and thermosetting matrices at high mass fractions. Composition and electrical properties of the composite samples are presented and related to the fibre structure in terms of CNT orientation and on the degree of infiltration of the polymer. The analysis of the prepared CNT fibre-based composites exhibited a modest improvement in the mechanical properties of the matrix and a high conductivity in the plane of the fibres. These CNT composite materials could find applications not only as direct structural elements, but due to their high electrical conductivity, also as interleaves for aerospace composite structures.

1. Introduction

An efficient route to exploit the properties of carbon nanotubes (CNT) is by pre-assembling the nanocarbon to form a macroscopic structure and then integrating it into a polymer matrix to fabricate composite using standard fibre-reinforced plastic (FRPC) manufacturing methods. CNT fibres can be produced by drawing an aerogel of CNTs directly from the gas-phase during CNT growth by chemical vapour deposition [1]. The process is based on using a high temperature reactor ($> 1000°C$), hydrogen as carrier gas, and often sulphur to control carbon diffusion [2], which results in very fast growth rates ($> 1mm/s$) of unusually long CNTs (around 1mm). Therefore, the gas-phase is constituted by entangled CNTs which form an aerogel that can be drawn out directly from the reactor as an *elastic smoke*. The material spun directly from the reactor is a low density diaphanous web which can be densified on-line through capillary forces after contact with a liquid [3] to form a fibre, or collected as a film.

The pristine fibres have low density, high specific surface and are highly porous. When embedded in a polymer matrix, the capillarity forces arising from the porous structure enables the infiltration of polymer molecules in the fibres; the formed composite acquires a complex hierarchical structure whose properties are not trivially related to those of the pristine fibres [4]. Reports on bulk properties of CNT fibre/epoxy composites indicate longitudinal specific tensile strengths around $250MPa$, electrical conductivity $10^4 S/m$ and thermal conductivity of $30W/mK$.

An innovative processing method was developed by X. Wang et al. [5] with the purpose of improving the multifunctional performance of CNT composites. The novelty of the process is that the CNT fibre was stretched and then embedded in the polymer matrix. The resulting composites were strong ($3.8GPa$), stiff ($293GPa$) and good thermal ($41W/mK$) and electrical ($1.23 \cdot 10^5 S/m$) properties.

The present work focuses on the preparation of CNT-fibre based composites and the study of their properties. Different polymer solutions were infiltrated in CNT-fibres.

2. Sample preparation

The CNT fibres used in this study were produced by floating catalyst chemical vapour deposition (CVD) [1]. 2-Butanol and ferrocene were used respectively as a carbon source and catalyst [6] and the furnace temperature was set to $1200°C$. Controlled growth of SWCNT was achieved by the addition of sulphur as a catalyst promoter [7] The fibre was used to prepare pre-impregnated (pre-preg) films. Polystyrene (PS), poly(methyl methacrylate) (PMMA) and 8552 epoxy resin films were used as matrices.

The production method was different depending on the choice of the polymer matrix, thermoplastic or thermosetting. In the case of thermoplastic matrices, both PS and PMMA, the fibre was collected on a polytetrafluoroethylene (PTFE) sustrate and subsequently impregnated with a solution of polymer in dichloromethane . The solvent was allowed to evaporate at room temperature (Figure 1(a)).In the case of thermosetting resins, the fiber was directly collected on a resin film and then intercaled between a second resin film layer, the multilayered film was heated at $130°C$ and $10KN$ during $300s$. Finally, the sandwich was frozen. Scheme of the protocol is depicted in Figure 1(b).

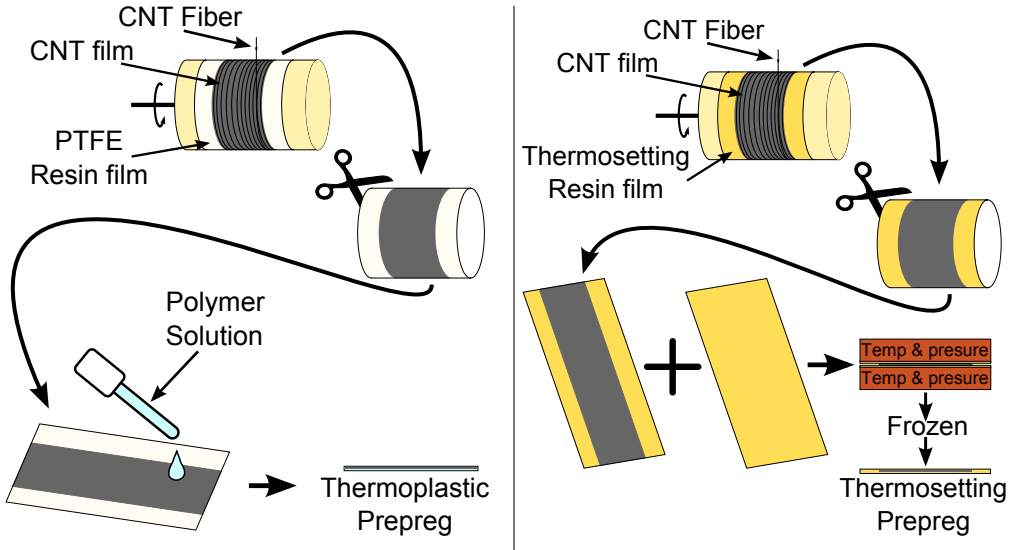

(a) Thermoplastic matrix (b) Thermosetting matrix

Figure 1. Scheme of how to do CNT fibre-based *prepregs*

All the prepared thermoplastic matrix composite and its abbreviations are listed in Table 1.

Description	Nomenclature
CNT Fiber noncondensed	CNTF-N
CNT Fiber condensed with DCM	CNTF-C
CNTF infiltrated with a solution of PMMA in DCM (concentration: 1 g/L)	1PMMA/CNTF
CNTF infiltrated with a solution of PMMA in DCM (concentration: 5 g/L)	5PMMA/CNTF
CNTF infiltrated with a solution of PS in DCM(concentration: 1 g/L)	1P/CNTF
CNTF infiltrated with a solution of PS in DCM(concentration: 5 g/L)	5PS/CNTF

Table 1. Thermoplastic matrix composites

3. Results

The thermosetting/termoplastic CNT-fibre composites have been characterized in order to obtain relevant information about their morphology (RAMAN, SEM and TEM), composition (TGA) electrical and mechanical properties.

3.1. Pristine fibre structure

The structure of the CNT fibre was analyzed by different techniques such as Raman spectroscopy, SEM and TEM.

The Figure 2 shows the Raman spectrum for the CNTF. The first important observation is the presence of RBM peaks, which only occurs when there are single or double walled nanotubes (SWCNTs and DWCNTs). In this case, four RBM peaks, at 153, 172, 182 and $274 cm^{-1}$ correspond to CNT diameters of 1.63, 1.44, 1.28 and $0.88 nm$ respectively, were observed. From these four values, $0.88 nm$ seems to be atypical and would correspond to thinner tubes. Since the interlayer distance between two graphene sheets is $0.34 nm$, a double wall CNT with the inner tube having a diameter of $0.88 nm$ would have an outer tube diameter of approximately $1.56 nm$, value that would lie around the other RBM values. This can be confirmed further by the lower Raman intensity of this peak, because of the restricted vibration that inner tubes present.

Additionally, the CNT fibre material was inspected by TEM (Figure 3). The catalyst presence was confirmed and the diameter of the CNTs were calculated to be around $1.4 nm$, which is consistent with the results obtained by Raman. Although forming bundles, the SWCNTs that make up the fibre provides a high specific surface (around $300 m^2/g$) and internal porosity accessible to small foreign molecules such as liquids and polymer.

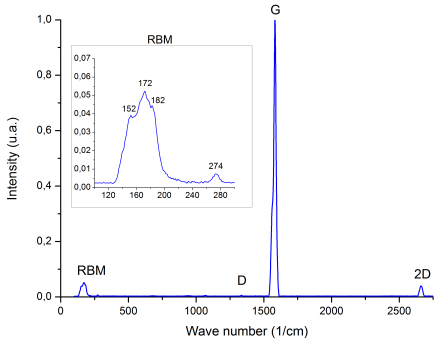

Figure 2. Raman spectra of different locations on a CNT fibre

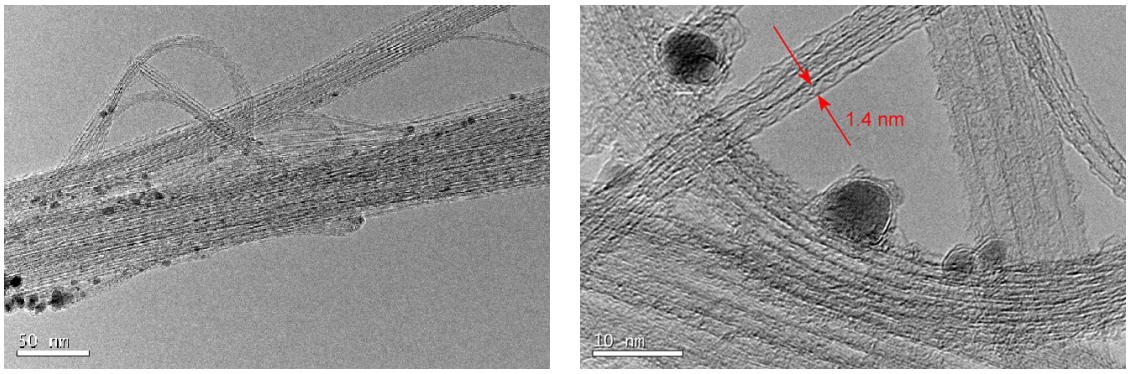

(a) General view (b) Detailed view

Figure 3. CNT fibre TEM images.

This porous structure can be clearly observed in Figure 4, consisting of sem micrographs of the fibre structure for as-spun (Figure 4(a)) and densified fibres (Figure 4(b)). The lack of cnt alignment is due to the low drawing rate of $7m/min$ used in this work, which was kept deliberately low to produce composites with isotropic properties in the plane.

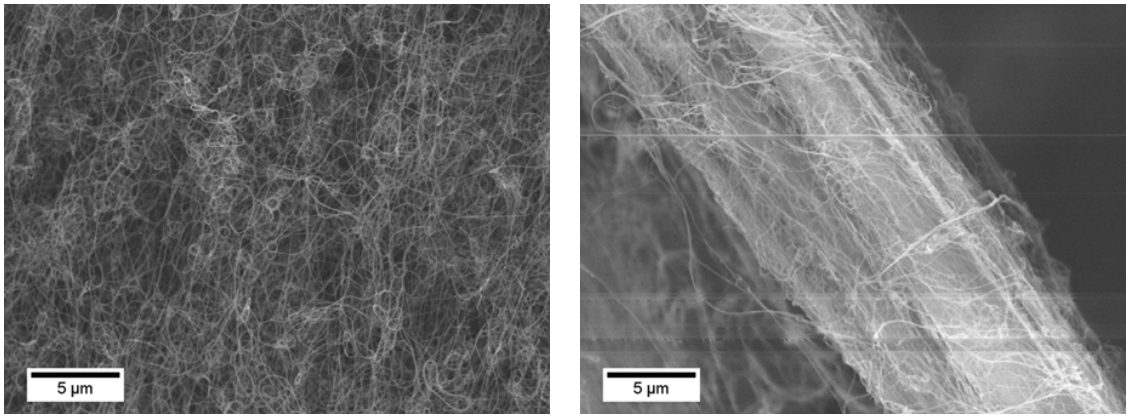

(a) Noncondensed carbon nanotube fibre (b) Condensed carbon nanotube fibre

Figure 4. CNT fibre SEM images.

3.2. Mass fraction

Thermogravimetric analysis (TGA) was used to determine the mass fraction of the CNT fiber in the composite. For this purpose, pristine CNT fibre, neat polymer and composite were analized. The Figure 5 compares the thermograms for pristine CNTF, neat PMMA and CNTF/PMMA composite. As can be seen, the degradation of PMMA starts at $225°C$ and has only one sharp and defined step. For the composites, another behavior was observed: two subsequent degradation steps could be distinguished, because the PMMA and CNTF degradation processes are decoupled. The iron content of the samples 1PMMA/CNTF and 5PMMA/CNTF was determined by the residue at $900°C$, being 11.5% and 10% respectively. When comparing the CNTF composites with the pristine fiber, it is also observed that the offset temperature of the CNT Fiber degradation was shifted towards higher temperature.

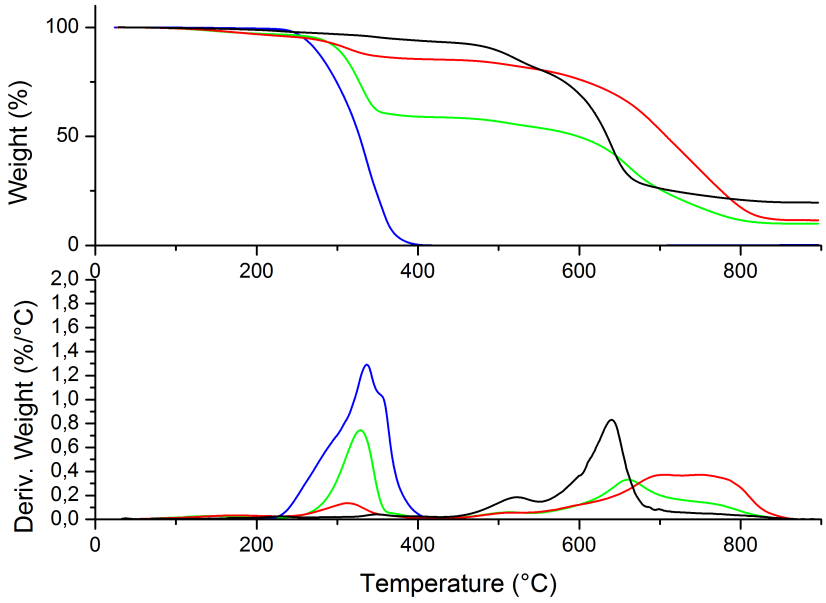

Figure 5. TGA and derivative curves of neat PMMA (blue), pristine CNTF (black), 1PMMA/CNTF (red) and 5PMMA/CNTF (green). $10°C/min$ and air atmosphere.

The TGA plots were used to determine the fiber mass fraction by Equation 1.

$$\begin{aligned} wt.\% &= A_1 f + B_1 m \\ wt.\% &= A_2 f + B_2 m \end{aligned} \tag{1}$$

Where wt.% corresponds to the observed mass fraction of the composite from room temperature through thermal decomposition, A_1 and B_1 correspond to the observed mass fraction for the pristine fiber and the neat polymer, respectively, evaluated at the same temperature. Finally, f and m represent the calculated mass fraction of CNTF and polymer respectively, present in the composite material. The values obtained following this method are summarized in Table 2

Composite	**wt.% of CNT fiber at** $430°C$	**wt.% of CNT fiber at** $880°C$
1PMMA/CNTF	91.4	58.8
5PMMA/CNTF	63.0	51.8
1PS/CNTF	96.3	68.3
5PS/CNTF	82.9	58.0

Table 2. wt.% of CNT fiber at different temperatures

3.3. Electrical resistance

The Figure 6 show as two pairs of square gold electrodes were deposited by physical vapour deposition (PVD) using a paper mask. The two-points resistance of the sample was measured between opposite electrodes, both parallel and perpendicular of spun direction. The data was treated following the Equation 2.

$$\rho = \frac{R \cdot a}{L} \tag{2}$$

Where R is the value of measurement, L ($20mm$) is the gap between opposite electrodes and a ($4mm$) is the electrode width.

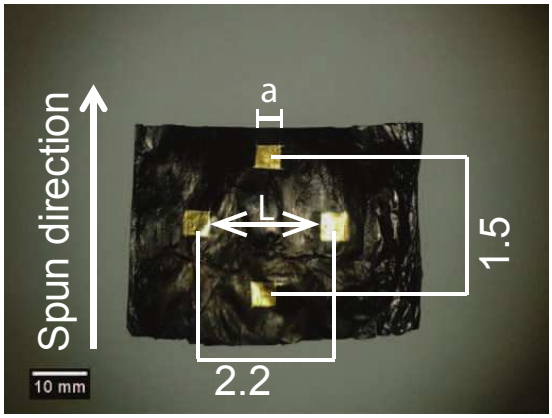

Figure 6. interleave of PMMA/CNTF specimen by electrical resistance measurements.

The results show that, in all cases, the surface resistance is higher across the width of the fibre than along the length of it. This anisotropy in electronic conduction is the preferential orientation of the carbon nanotubes along the fibre winding direction (drawing out the furnace). The fibre presented slightly lower surface resistance when densified (Figure 7(a)), due to increased contact between CNTs after capillary densification . Finally, from the samples infiltrated with PS and PMMA, with the same solvent and concentration, the PMMA one exhibited higher surface resistance (Figure 7(b)). This phenomenon can be explained because the PMMA samples have a higher quantity of polymer (determined by TGA). These polymer composites show a very low anisotropy ($2.2\Omega, 1.5\Omega$), like the pure CNT fibre. In addition the resistance through thickness is 0.22Ω, which assuming $25\mu m$. These properties are ideal for interleaves used in aerospace composite structures.

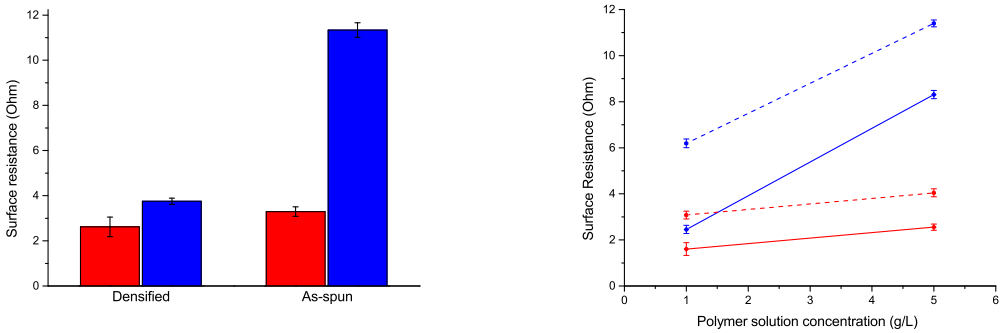

(a) Pure CNT fibre

(b) PS/CNTF (continuous line) and PMMA/CNTF (dashed line)

Figure 7. Electrical resistance along the length (red) and perpendicular of the fibre (blue) in pure state and in polymer composite

4. Conclusions

The Raman analysis and SEM images shows that the structure of different batches of CNTF produced in same conditions have similar morphologies. Moreover, the as-produced fibre had superior properties along the winding direction, due to preferential alignment in the drawing direction, although when inspected the electrical resistance of the fibre (Figure 7), it was found a low anisotropy degree of the measurement proved the the lack of a high alignment. This was further confirm by SEM (Figure 4).

The polymers used in this work are electrical insulators, therefore an electrical resistance increase will be expected when higher amounts of polymer are infiltrated in the CNTF. When the comparison is done between the pristine CNTF and the polymer infiltrated fibre, the electrical resistance barely changes, especially along the fibre length. This can be explained because at the CNTF fibre the percolating network of CNTs is formed and the polymer infiltration does not affect their interconnections. An additional reason for maintaining a high electrical conductivity and a low degree of anisotropy is that this fibre consists mainly of SWCNT, so that the specific surface is very high, hence has a high probability of contact.

References

[1] Ya-Li Li, Ian A. Kinloch, and Alan H. Windle. Direct spinning of carbon nanotube fibers from chemical vapor deposition synthesis. *Science*, 304(5668):276–278, 2004.

[2] M. S. Motta, A. Moisala, I. A. Kinloch, and A. H. Windle. The role of sulphur in the synthesis of carbon nanotubes by chemical vapour deposition at high temperatures. *Journal of Nanoscience and Nanotechnology*, 8(5):2442–2449, 2008.

[3] Krzysztof Koziol, Juan Vilatela, Anna Moisala, Marcelo Motta, Philip Cunniff, Michael Sennett, and Alan Windle. High-performance carbon nanotube fiber. *Science*, 318(5858):1892–1895, 2007.

[4] Juan J Vilatela, Rupesh Khare, and Alan H Windle. The hierarchical structure and properties of multifunctional carbon nanotube fibre composites. *Carbon*, 50(3):1227–1234, 2012.

[5] X Wang, Z Z Yong, Q W Li, P D Bradford, W Liu, D S Tucker, W Cai, F G Yuan, and Y T Zhu. Ultrastrong , Stiff and Multifunctional Carbon Nanotube Composites. *Materials Research Letters*, 1(1):19–25, 2013.

[6] M. Bystrzejewski, A. Huczko, P. Byszewski, M. DomaÅska, M. H. Rümmeli, T. Gemming, and H. Lange. Systematic Studies on Carbon Nanotubes Synthesis from Aliphatic Alcohols by the CVD Floating Catalyst Method. *Fullerenes, Nanotubes and Carbon Nanostructures*, 17(3):298–307, May 2009.

[7] V. Reguero, B. Aleman, B. Mas, and J.J. Vilatela. Submmited.